Supporting Information

Dynamical control over terahertz electromagnetic interference shielding with 2D $Ti_3C_2T_y$ MXene by ultrafast optical pulses

Guangjiang Li[1,], Naaman Amer[2,*], Hassan A. Hafez[3], Shuohan Huang[4], Dmitry Turchinovich[3], Vadym N. Mochalin[4,5,&], Frank A. Hegmann[2], Lyubov V. Titova[1,#]*

[*] *These authors contributed equally*

[1] *Department of Physics, Worcester Polytechnic Institute, Worcester, MA 01609, USA*

[2] *Department of Physics, University of Alberta, Edmonton, AB T6G 2E1, Canada*

[3] *Fakultät für Physik, Universität Bielefeld, 33615 Bielefeld,Germany*

[4] *Department of Chemistry, Missouri University of Science & Technology, Rolla, MO 65409, USA*

[5] *Department of Materials Science & Engineering, Missouri University of Science & Technology, Rolla, MO 65409, USA*

[&] mochalinv@mst.edu

[#] ltitova@wpi.edu

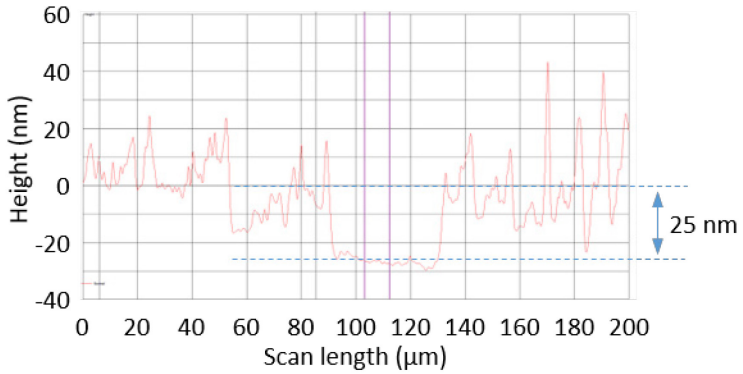

Figure S1. Profilometer (P-7 stylus profiler, Kla Tencor) scan over a region where the film was removed down to the substrate. Average film thickness is 25 nm.

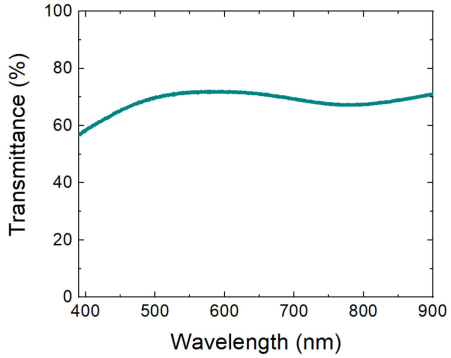

Figure S2. UV-VIS optical transmittance of the film.

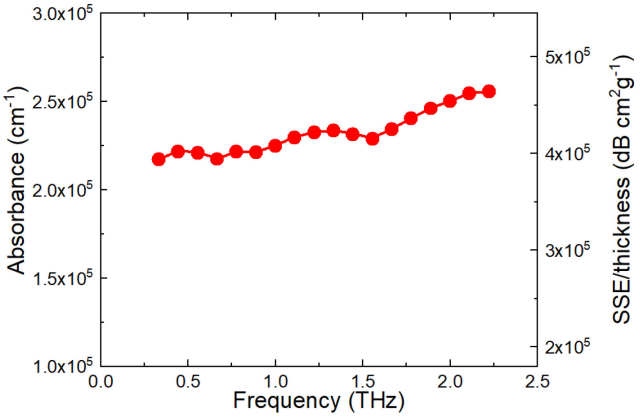

Figure S3. THz absorbance (left) and corresponding specific EMI shielding per unit thickness, defined as SE divided by density and thickness (right) for a $Ti_3C_2T_y$ film.

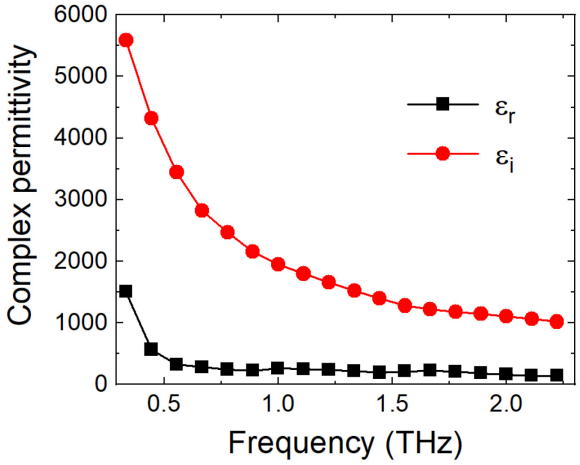

Figure S4. Complex permittivity (black squares – real permittivity, and red circles – imaginary permittivity) for a $Ti_3C_2T_y$ film.

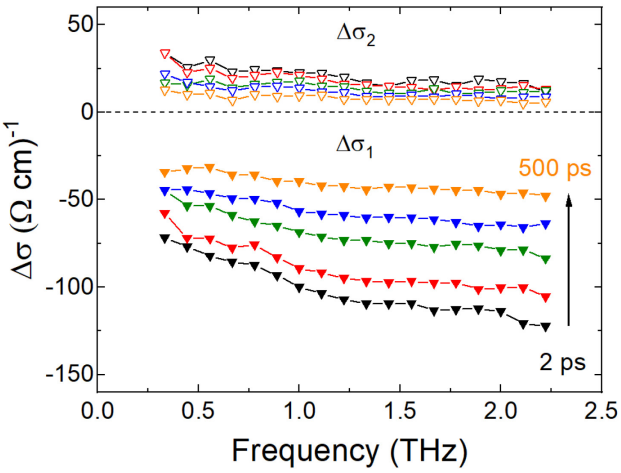

Figure S5. Photoinduced change in real (solid symbols) and imaginary (open symbols) conductivity as different times after excitation with 800 nm, 950 μJ/cm^{2}pulse at 290 K.

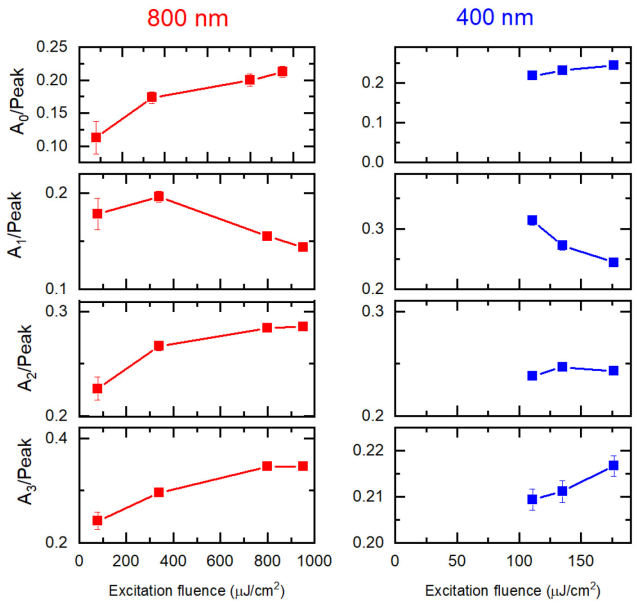

Figure S6. Fitting parameters resulting from fitting decays of photoinduced THz transmission enhancement to a three exponential decay function: $A_0/Peak$, $A_1/Peak$, $A_2/Peak$, and $A_3/Peak$ are decay amplitudes weighted by the peak of the THz transmission enhancement to provide relative contribution of different decay components to the relaxation of the photoinduced THz transmission enhancement.

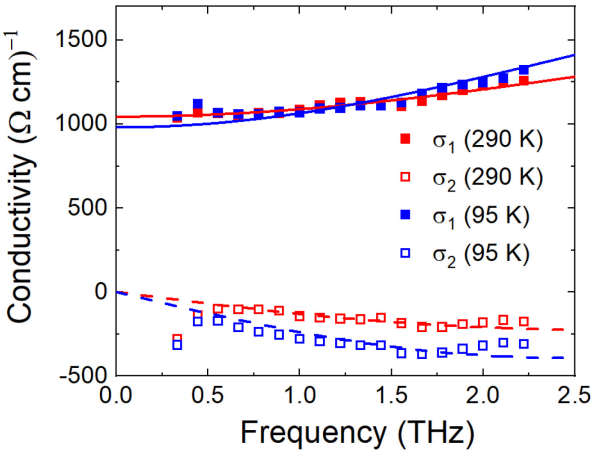

Figure S7. Complex THz conductivity (solid symbols represent real and open symbols – imaginary conductivity components; lines show a global fit of both components to the Drude-Smith model) at 290 K (red) and 95 K (blue).

We find that the real component of intrinsic THz conductivity does not change between 290 K and 95 K. A small change in imaginary component seen in Figure S3 results in a small (22 ± 1 fs vs 19 ± 1 fs) increase

in carrier scattering time within the nanoflakes, consistent with a small decrease in carrier-phonon scattering, accompanied by a small change in the Drude-Smith c-parameter (-0.745 ± 0.008 vs -0.68 ± 0.04) which can be ascribed to a suppressed inter-flake transport. However, small artificial negative contributions to the imaginary conductivity can also arise from small (~ 10 fs) errors in the measured phase due to variation of the substrate thickness.[1-2] Regardless of the origin of the observed negative imaginary conductivity, only real conductivity component impacts power absorption,[3] and is therefore relevant to the discussion of EMI SE.

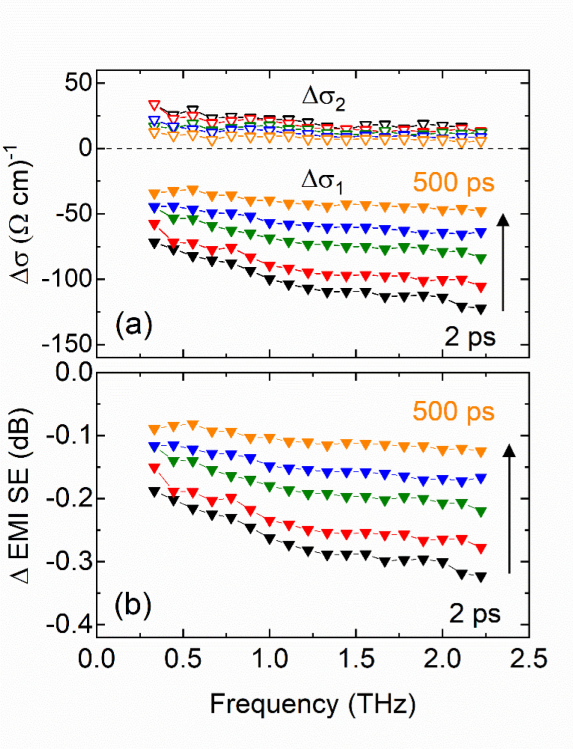

Figure S8. Photoinduced change in (a) real (solid symbols) and imaginary (open symbols) conductivity and (b) EMI SE at different times after excitation with 800 nm, 950 μJ/cm²pulse at 95 K.

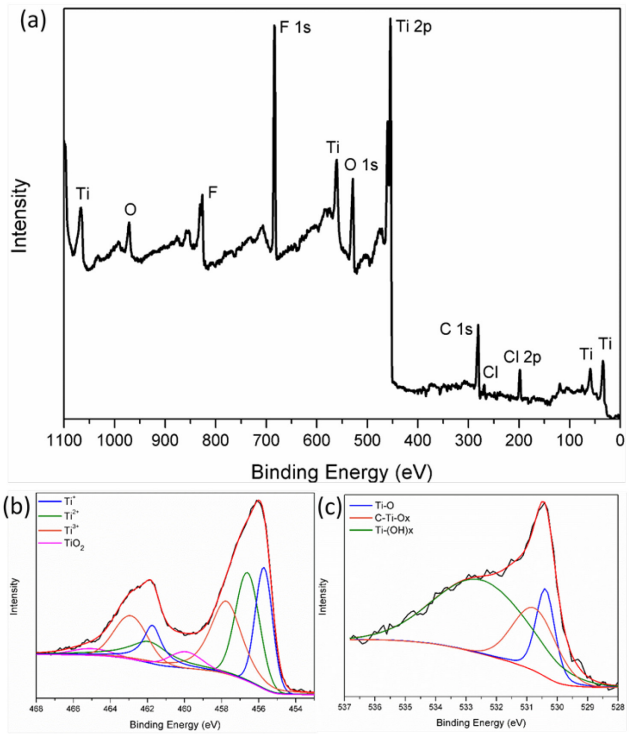

Figure S9 *(a) XPS survey for $Ti_3C_2T_y$ MXene. High-resolution XPS spectra of $Ti_3C_2T_y$ MXene for (b) Ti 2p and (c) O 1s.*

XPS investigation was performed to characterize the surface chemistry of the prepared $Ti_3C_2T_y$ MXene. The survey spectrum in Figure S9a shows the presence of Ti, O, F, C and small amount of Cl. The high-resolution XPS spectrum of Ti 2p is shown in Figure S9b. The peaks at binding energies of 455.7 and 461.7 eV, 456.6 and 461.9 eV, 457.7 and 462.9 eV as well as 459.9 and 465.0 eV can be assigned to Ti^{+}, Ti^{2+}, Ti^{3+} and TiO_2, respectively. Similarly, the O 1s spectrum is shown in Figure S9c with the Ti-O peak at 530.4 eV, the C-Ti-O_x peak at 530.7 eV and the Ti-$(OH)_x$ peak at 532.5 eV. The summary of the high-resolution Ti 2p and O 1s XPS regions is provided in Table S1.

Table S1. Summary of the high-resolution Ti 2p and O 1s XPS regions of $Ti_3C_2T_y$ MXene

	Peak Position (eV)	Area (%)	FWHM (eV)
Ti	455.7 (3/2)	17.45	1.10
	461.7 (1/2)	8.73	1.19
	456.6 (3/2)	21.28	1.51
	461.9 (1/2)	10.64	2.64
	457.7 (3/2)	23.60	2.00
	462.9 (1/2)	11.80	2.10
	459.9 (3/2)	4.33	2.04
	465.0 (1/2)	2.17	2.48
O	530.4	16.25	0.74
	530.7	23.66	1.69
	532.5	60.09	3.65

References

(1) Schneider, A. Terahertz characterization of semiconductor alloy AlInN: negative imaginary conductivity and its meaning: comment. *Opt. Lett.* **2010,** *35* (2), 265-265, DOI: 10.1364/OL.35.000265.
(2) Alberding, B. G.; Kushto, G. P.; Lane, P. A.; Heilweil, E. J. Reduced photoconductivity observed by time-resolved terahertz spectroscopy in metal nanofilms with and without adhesion layers. *Appl. Phys. Lett.* **2016,** *108* (22), DOI: 10.1063/1.4953208.
(3) Dressel, M.; Grüner, G. *Electrodynamics of Solids: Optical Properties of Electrons in Matter*, Cambridge University Press: Cambridge, 2002.